


 Cite this: *RSC Adv.*, 2023, 13, 2427

# Sustainable solvents for $\beta$ -diketone extraction from wheat straw wax and their molecular self-assembly into nano-structured tubules for hydrophobic coatings†

 Pakin Noppawan,<sup>a</sup> Suwivat Sangon,<sup>b</sup> Petcharaphorn Chatsiri,<sup>bc</sup>  
 Nutnicha Khunmood,<sup>bd</sup> Suphatta Aintharabunya,<sup>b</sup> Nontipa Supanchaiyamat<sup>id</sup><sup>b</sup>  
 and Andrew J. Hunt<sup>id</sup><sup>\*b</sup>

Nonpolar, nonperoxide forming, sustainable and potentially bio-based solvents, namely 2,2,5,5-tetramethyloxolane (TMO) and 2,5-diethyl-2,5-dimethyloxolane (DEDMO), were utilized as an alternative to toxic petroleum-based hydrocarbon solvents for extraction of hentriacontane-14,16-dione from waste wheat straw waxes. This work is the first to report the application of DEDMO as a solvent for the extraction of natural products. The sustainable methodology developed in this research provided considerable advantages over previously reported systems in terms of high extraction yields, excellent selectivity towards the  $\beta$ -diketones and low amounts of waste generated. DEDMO provided the highest recovery yield for all the sustainable solvents investigated, recovering 23.7% of the wax (which is a 68.8% yield of the  $\beta$ -diketone). The extracted lipophilic hentriacontane-14,16-dione was utilised in combination with the sustainable solvents TMO or DEDMO to facilitate the creation of highly hydrophobic coatings. Moreover, the use of DEDMO was found to aid in the self-assembly of nano-structured tubule formation of both the unrefined wax and isolated  $\beta$ -diketone. Green metric evaluation using process mass intensity (PMI), E-factor, solvent intensity (SI), and water intensity (WI) demonstrated that the described extraction procedure for hentriacontane-14,16-dione was highly sustainable and safer than the previous methodology. This sustainable manufacturing process may create the potential to valorise agricultural wastes as part of a holistic biorefinery.

 Received 29th November 2022  
 Accepted 19th December 2022

DOI: 10.1039/d2ra07581d

[rsc.li/rsc-advances](https://rsc.li/rsc-advances)

## 1. Introduction

Global policy has shifted towards using biomass as a local, renewable, and low-carbon footprint feedstock since the 1990s, as a result of diminishing fossil fuel sources, rising oil prices, concerns about supply security, and environmental effects.<sup>1</sup> A biorefinery is analogous to modern petroleum refineries, it utilizes biomass to create a variety of value-added products, including energy, chemicals, and materials in an integrated facility.<sup>1</sup> However, first-generation biorefineries use feedstocks

in which directly compete with food applications.<sup>2</sup> The use of lignocellulosic agricultural residues, which do not compete with food, and food supply chain (FSC) wastes, can help create flexible zero-waste networks.<sup>3</sup> Utilizing such wastes can result in the creation of inventive ranges of products that can satisfy the needs of both established and emerging sectors.<sup>3</sup> There is a wide range of lignocellulosic materials that are suitable feedstocks for a biorefinery, with different concentrations of lignin, cellulose, and hemicellulose. Waste agricultural residues are one such feedstock that has received significant attention. Additionally, these materials have the capacity to offer a sophisticated mixture of phytochemicals that could be useful in high-value applications.

Wheat straw has excellent potential as a low value, an abundant feedstock from wheat production for biorefineries.<sup>1,4</sup> With more than 2 million hectares planted in wheat, the EU produces a significant number of cereal crops. In the UK alone, this crop produces almost 7.5 million tonnes of straw each year.<sup>5</sup> In 2016, the globe produced more than 2.8 billion tons of cereals, with wheat (*Triticum*) being one of the most extensively grown crops.<sup>6</sup> The annual production of wheat surged by nearly

<sup>a</sup>Department of Chemistry, Faculty of Science, Mahasarakham University, Maha Sarakham, 44150, Thailand

<sup>b</sup>Materials Chemistry Research Center, Department of Chemistry and Center of Excellence for Innovation in Chemistry, Faculty of Science, Khon Kaen University, Khon Kaen, 40002, Thailand. E-mail: andrew@KKU.ac.th

<sup>c</sup>Vidyasirimedhi Institute of Science and Technology (VISTEC), Rayong, 21210, Thailand

<sup>d</sup>Agilent Technologies, 22nd Floor, U Chu Liang Bldg, Rama IV Road, Bangrak, Bangkok, 10500, Thailand

† Electronic supplementary information (ESI) available. See DOI: <https://doi.org/10.1039/d2ra07581d>



200 million tons from 1986 to 2016, surpasses 700 million tons every year. Among the major producers, the United States and Canada produce an average of 85 million tons of wheat in 2016.<sup>6</sup> According to FAO 2018, there was a global production of 755.8 million tons of wheat grain in 2016–2017, which results in an average amount of 1.3–1.4 kg of wheat straw per kg of wheat grain.<sup>7</sup>

An integrated biorefinery's first step should include the extraction of important secondary metabolites or natural products.<sup>1</sup> Wheat straw has a significant amount of lipids around 1–2 percent by weight that could be extracted to create higher-value products, however frequently such molecules are overlooked or under exploited.<sup>8</sup> Natural waxes are used in a variety of commercial products, including polishes, coatings, personal care items, and cosmetics.<sup>7,9</sup>

$\beta$ -Diketones are frequently a component in plant cuticle wax and are an intriguing class of molecules present in wheat straw extracts.  $\beta$ -Diketones have been found in a wide variety of other cereal crops, including barley, oat, and flax.<sup>10–12</sup> According to previous studies,<sup>9,13</sup> hentriacontane-14,16-dione (C31) is one of the main lipid components found in wheat straw wax and has been widely described as the key  $\beta$ -diketone in young wheat plants.<sup>14–17</sup>

Traditionally, waxes are extracted using hexane and other volatile organic solvents. These solvents are harmful to the environment, poisonous, and unselective.<sup>9,13</sup> In accordance to the definitions provided by the Registration, Evaluation, and Restriction of Chemicals (REACH) regulation, the European Chemical Agency (ECHA) identified *n*-hexane as suspected of harming fertility or the unborn child.<sup>18</sup> It is also regarded as a hazardous air pollutant by the United States Environmental Protection Agency (US EPA).<sup>19</sup>

Over the past few years, green solvent extractions such as subcritical and supercritical fluids have been thoroughly researched and refined to give a better understanding of the wax yields and selectivity associated with these techniques.<sup>20–25</sup> Sin *et al.* reported that hentriacontane-14,16-dione was extracted from wheat straw wax by supercritical carbon dioxide (scCO<sub>2</sub>) in a yield of 34.5% of the wax.<sup>26</sup> Importantly, scCO<sub>2</sub> processes have demonstrated effectiveness at the extraction of waxes, however, to date scCO<sub>2</sub> fractionations are yet to demonstrate selectivity in the isolation of  $\beta$ -diketones.

Canizares *et al.*<sup>13</sup> also reported hentriacontane-14,16-dione was the major compound found in wheat straw waxes, with significantly higher  $\beta$ -diketone yields of between 62.9 to 66.8% for epicuticular wax. These were obtained by repeated immersion in liquid nitrogen, while a 40% yield of  $\beta$ -diketone from cuticular wax was also observed by immersion in *n*-hexane. The use of liquid nitrogen as an extraction system is a highly energy-intensive process and has a limited application on an industrial scale. In contrast, solvent extraction with hexane and other traditional solvents are commonly utilised at scale, however, the use of such solvents possesses significant health and environmental concerns. As such, sustainable approaches are still required for the effective fractionation of molecules such as  $\beta$ -diketones.

Chelation of hentriacontane-14,16-dione with copper has been utilized as an efficient method for  $\beta$ -diketone recovery. With the aid of Cu(OAc)<sub>2</sub>, it is of great interest to be able to create metal chelates, thereby enabling  $\beta$ -diketones isolation and opening a potential market for these molecules. A metal ion can take the place of the enolic hydrogen in  $\beta$ -diketones through a process known as keto–enol tautomerism, which results in the formation of a chelate ring.<sup>27</sup> Hentriacontane-14,16-dione has been proven to be an excellent chelator and can be easily separated from the rest of the wheat straw wax by chelating to copper(II) salts to create insoluble copper complexes (Scheme S1†).<sup>28</sup>

Asemave and co-workers<sup>29</sup> reported precipitating lipophilic  $\beta$ -diketone from a variety of solutions, including petroleum ether, cyclohexane, *p*-cymene, and cyclopentyl methyl ether (CPME) of plant wax. However, petroleum ether and cyclohexane are petroleum-based or regarded as toxic solvents. Additionally, green solvents including, *p*-cymene and CPME provided low product recovery. Although 2,2,5,5-tetramethyloloxane (TMO) was investigated and yielded the greatest recovery yield of  $\beta$ -diketones at 21.40 wt%, however, the major drawback of the method is the extensive volumes of solvents and chemical used. The long-term sustainability of elements are causing growing environmental concerns and as such it is vital to develop efficient processes.<sup>30,31</sup>

The hydrophobic qualities of  $\beta$ -diketones can also be used in industrial applications. There are many plants that offer superhydrophobic or self-cleaning qualities that limit water loss and inhibit the adherence of debris or potential infections.<sup>32</sup> These hydrophobic materials can be applied to a variety of bio-inspired products, such as self-cleaning windows, textiles, and packaging. Because of the potential for widespread applications in self-cleaning, drag reduction, anti-sticking, anti-icing, and other areas, there has been a lot of interest in understanding the superhydrophobicity of plant surfaces.<sup>33–40</sup> The leaves of the *Nelumbo nucifera* or Lotus plant, which have a hierarchical structure made of convex cell papillae and randomly oriented hydrophobic wax tubules overlaid, serve as a model surface for superhydrophobicity and self-cleaning.<sup>41–43</sup> The wax crystals are generated by a self-assembly process, and frequently one component of the wax is responsible for the structuring of the wax.<sup>44–47</sup> The primary forms of wax are crusts, platelets, plates, rodlets, threads, and tubules. Secondary alcohol tubules and  $\beta$ -diketone tubules are two further classifications of tubules based on their primary component. The high amount of  $\beta$ -diketone, such as hentriacontane-14,16-dione, tubules are reported as having a diameter of 0.2–0.3  $\mu$ m and a length of 2–3  $\mu$ m.<sup>47</sup> In addition, it is possible that the waxes' natural chemical and physical properties, as well as the solvents, can affect how wax structure forms.<sup>37,44,48,49</sup> Thus potentially affecting their hydrophobic properties.

Herein, this research focuses on the utilization of sustainable and potentially bio-based solvents for the replacement of hazardous hydrocarbon solvents in the extraction of high-value  $\beta$ -diketone, hentriacontane-14,16-dione from wheat straw wax through the application of green methodologies. The effect of sustainable solvents on the molecular self-assembly of nano-



structured hentriacontane-14,16-dione tubules, as well as their hydrophobicity was also investigated. The use of sustainable solvents could significantly expand the field of plant wax extraction in the future, by offering a safe, environmentally friendly, and cost-effective substitute for harmful petroleum-based solvents.

## 2. Experimental

Unless otherwise stated, all reagents and solvents were used as obtained from commercial sources without purification. H-beta zeolite (25 : 1) was supplied by Alfa Aesar. TMO and DEDMO were synthesized following literature procedures,<sup>50,51</sup> by the ring closure dehydration of 2,5-dimethyl-2,5-hexanediol (purchased from Sigma-Aldrich) for TMO and 3,6-dimethyl-3,6-octanediol for DEDMO in the presence of H-beta zeolite (25 : 1). Infrared (IR) spectrum was measured on a Bruker tensor 27 Fourier-transform infrared (FT-IR) spectrophotometer. The nuclear magnetic resonance (NMR) spectra (<sup>1</sup>H NMR and <sup>13</sup>C NMR) in this work were recorded on a Bruker Avance Neo 400 MHz spectrometer in CDCl<sub>3</sub>. The NMR data were processed and analysed by MestReNova software. The morphology of recrystallized hentriacontane-14,16-dione were investigated using scanning electron microscopy (LEO 1450 VP Scanning Electron Microscope).

### 2.1. Determination of the Kamlet–Taft parameters ( $\pi^*$ ) of petroleum ether

The determination of the  $\pi^*$  Kamlet–Taft parameter was performed in the same manner as previously described with *N,N*-diethyl-4-nitroaniline.<sup>50</sup>

### 2.2. GC-FID for analysis of hentriacontane-14,16-dione

An Agilent 7890B gas chromatograph with flame ionization detector (GC-FID), fitted with a HP-5 capillary column (30 m x 32  $\mu$ m x 0.25  $\mu$ m film thickness) was used in this work. Helium was used as the carrier gas at flow rate of 1.2 mL min<sup>-1</sup> with constant pressure of 22.35 psi. The sample were injected at 290 °C with a split ratio of 50 : 1. Oven temperature starts at 50 °C and held for 4 min, then ramped at 10 °C min<sup>-1</sup> and finally reaches to 290 °C and held for 10 min. The detector temperature was 340 °C. The total time was 38.0 min.

### 2.3. GC-MS for analysis of hentriacontane-14,16-dione

A gas chromatograph-mass spectrometry (GC-MS) proceeded on an Agilent 8890 gas chromatograph equipped with 5977B mass spectrometer. The equipment was equipped with a HP-5MS ultra inert fused silica capillary column coated with 5% phenylmethylpolysiloxane (30 m x 250  $\mu$ m x 0.25  $\mu$ m film thickness). The carrier gas utilized in GC-MS was helium with flow rate at 1.2 mL min<sup>-1</sup>, and the split ratio used was 50 : 1. The temperature of the injector was 300 °C. The oven temperature was maintained at 60 °C and held for 1 min. The temperature increased at rate 10 °C min<sup>-1</sup> until 300 °C and held for 10 min. The Clarus 500 quadrupole mass spectrum was conducted in electron ionization (EI) mode at 70 eV with the source

temperature of 300 °C, quadrupole at in the scan range of 30–1200 amu s<sup>-1</sup>.

### 2.4. Extraction of hentriacontane-14,16-dione from wheat straw wax

Hentriacontane-14,16-dione was recovered from dried wheat straw wax by liquid–liquid extraction using petroleum ether (40–60 °C), toluene, and sustainable solvents *i.e.*, 2,2,5,5-tetra-methyloxolane (TMO) and 2,5-diethyl-2,5-dimethyl-oxolane (DEDMO). The ratio of wax to solvent was varied from 1 : 30, 1 : 60, 1 : 100, 1 : 150, and 1 : 300. To preliminary the feasibility of the solvents for hentriacontane-14,16-dione extraction *i.e.*, in case of 1 : 300 of wax to the solvent system: 1 g of wheat straw wax was crushed with a spatula in a beaker and dissolved in 200 mL of solvent. The mixture was stirred at room temperature for 30 min and transferred to a separatory funnel, followed by the addition of 100 mL hot excess saturated aqueous Cu(OAc)<sub>2</sub>. Then the mixture was shaken for 20 min and allowed to stand for 1 hour. The organic phase becomes green, while the aqueous phase become light blue with a dark blue of Cu–diketones in between the two phases. The system was heated with a heat-gun to afford proper separation. The aqueous layer was removed and the organic phase that contained Cu–diketone complex was collected and kept for 2 hours at room temperature followed by refrigeration at 4 °C for 2 or 4 hours, thus enabling the complete precipitation of the Cu–diketones complex. The precipitate was then filtered and washed with 5 mL of extraction solvent. The copper salt was re-dissolved in 100 mL of hot chosen solvent and transferred to a separating flask followed by the addition of 2 mL of hydrochloric acid. The mixture was shaken for 10 min to strip out the Cu(II) ions from hentriacontane-14,16-dione in the organic phase and washed with deionized distilled water. The product was recovered from the organic layer by removing the solvent under a vacuum in a rotary evaporator. The other ratio of wax to solvent systems was performed in the same procedure (Table S1†). The extraction procedure of the extraction of hentriacontane-14,16-dione from wheat straw wax is shown in Fig. S1.† The recovery yield of hentriacontane-14,16-dione was calculated in term of dried matter as describe in equation below.

$$\text{Recovery(\%)} = \frac{\text{weight of hentriacontane-14, 16-dione (g)}}{\text{weight of dried wheat straw wax (g)}} \times 100$$

## 3. Results and discussion

### 3.1. Extraction of 14,16-hentriacontanedione from wheat straw wax

Hentriacontane-14,16-dione was firstly purified from wheat straw wax using petroleum ether with cuprous acetate by Asemave and co-workers.<sup>28</sup> They reported the use of a total of 300 mL of petroleum ether per 1 g of wheat straw wax to isolate hentriacontane-14,16-dione and can recover only 18% of the product. In this current work, the isolation of the  $\beta$ -diketones from wheat straw wax was also achieved using the chelation



ability of the molecule. Significant method modifications, and optimization was undertaken to increase the efficiency and yields of the desired product. Hentriacontane-14,16-dione was extracted using traditional solvents including petroleum ether and toluene, as well as the sustainable and potentially bio-based solvents, TMO and DEDMO. All these solvents can dissolve the wheat straw wax and the precipitation of hentriacontane-14,16-dione was carried out by contacting with hot unsaturated cuprous acetate in a biphasic system. The Cu-diketone complex was formed and accumulated at the interphase of the organic/water system as a dark blue layer. The free hentriacontane-14,16-dione was obtained from Cu-diketone by subsequent filtration, redissolution in a fresh solvent and stripping with concentrated hydrochloric acid.

This work utilizes a wax containing 34.5% hentriacontane-14,16-dione, therefore the yield of isolated the  $\beta$ -diketone was calculated based on this composition. To optimize the extraction conditions, various parameters including volume of the solvent, precipitation temperature, and the type of solvent used for extraction are vital to enable to precipitation of hentriacontane-14,16-dione with a standard deviation of less than 0.5%, Table 1 (see ESI† for full optimization). Under the optimal conditions, the total amount of petroleum ether used can be reduced from 300 mL to 30 mL (a tenfold reduction in solvent use), and the recovered desired product was up to 24.4% (70.6% yield). In the diketone precipitation process with Cu, refrigeration for 4 hours promoted the Cu-diketone complex formation and isolation, leading to an increased yield.

TMO gave 21.8% hentriacontane-14,16-dione from the wax or a 63.1% yield, which is comparable to those achieved in toluene (21.9% recovery and 63.6% yield). TMO has proven to be a more environmentally friendly substitute for toluene.<sup>50</sup> It exhibits low polarity, does not produce dangerous peroxides, and has a similar boiling point to toluene ( $T_b = 112$  °C compared to 111 °C for toluene).<sup>50</sup> Although the extraction of hentriacontane-14,16-dione by using TMO using the optimized method was comparable to previous reports (21.4% recovery), it demonstrated a tenfold reduction in solvent use.<sup>29</sup>

A newly developed sustainable and potentially bio-based solvent, namely DEDMO, is a promising alternative to traditional toxic nonpolar solvents such as toluene and hexane.<sup>51</sup> DEDMO contains two ethyl groups in the structure that promoted the nonpolar character compared to TMO and provided better extraction performance for lipophilic

**Table 1** Extraction of hentriacontane-14,16-dione from wheat straw wax under optimal conditions using different solvents

| Solvent         | Recovery (%) | Yield (%) <sup>a,b</sup> |
|-----------------|--------------|--------------------------|
| Petroleum ether | 24.4         | 70.6                     |
| Toluene         | 21.9         | 63.6                     |
| TMO             | 21.8         | 63.1                     |
| DEDMO           | 23.7         | 68.8                     |

<sup>a</sup> Calculated based on the composition of hentriacontane-14,16-dione from Sin's report (34.5%).<sup>26</sup> <sup>b</sup> Standard deviation less than 0.5%.

compounds similar to non-polar petroleum ether. When using DEDMO, hentriacontane-14,16-dione was extracted at an amount of 23.7% (68.8% yield), which was comparable to that of petroleum ether. This is also confirmed the less polar properties of DEDMO. Comparing the sustainable solvents (TMO and DEDMO) in this work to other green solvents (*p*-cymene and CPME) from previous work,<sup>29</sup> TMO and DEDMO provided superior recovery yield of hentriacontane-14,16-dione compared to those obtained from *p*-cymene (8.2%) and CPME (7.8%).

The CHEM21 solvent selection criteria were used to evaluate the green credentials of both traditional and sustainable solvent extraction.<sup>52</sup> These were also compared to green solvents previously reported (*p*-cymene and CPME).<sup>29</sup> A three-tiered assessment of safety, health, and environmental effect (SH&E), with scores ranging from 1 to 10, was used to classify the solvents according to the hazard levels (Table 2). The original CHEM21 report did not list solvents such as petroleum ether, TMO, and DEDMO, but by using the physical data and hazard information taken from Safety Data Sheets,<sup>52</sup> these solvents could be assigned the SH&E scores. Overall, except for petroleum ether, which is classified as hazardous, most of the solvents represent a problematic ranking. TMO, and DEDMO have a health score of 5 by default because they have not yet been REACH registered. According to REACH Annex V, petroleum ether has been exempted from registration due to it is a mixture of hydrocarbons.<sup>53</sup> The designation of CPME as "problematic" is due to its resistivity in relation to the low auto-ignition point (180 °C).<sup>52</sup> Although it was discovered that TMO's boiling point (112 °C) and toluene's (111 °C) were very similar, TMO obtained a yellow-shaded environmental score of 5 and toluene received a green-shaded environmental score of 3, as TMO has not yet been registered in REACH.<sup>52</sup> Therefore, the CHEM21 solvent guide suggests that TMO and DEDMO could be more environmentally friendly than other solvents, however, REACH registration would need to be conducted to realize such potential.<sup>52</sup>

**Table 2** CHEM21 solvent guide of solvents<sup>52</sup>

| Solvent          | BP (°C) | Worst H3xx <sup>d</sup> | H4xx | S <sup>a</sup> | H <sup>b</sup> | E <sup>b</sup> | Ranking <sup>c</sup> |
|------------------|---------|-------------------------|------|----------------|----------------|----------------|----------------------|
| Petroleum ether  | 40–60   | H361                    | H411 | 7              | 7              | 7              | Hazardous            |
| Toluene          | 111     | H351                    | None | 5              | 6              | 3              | Problematic          |
| TMO              | 112     | n.a.                    | n.a. | 1              | 5              | 5              | Problematic          |
| DEDMO            | 162     | n.a.                    | n.a. | 1              | 5              | 5              | Problematic          |
| <i>p</i> -Cymene | 177     | H331                    | H411 | 4              | 6              | 7              | Problematic          |
| CPME             | 106     | H302                    | H412 | 7              | 2              | 5              | Problematic          |

<sup>a</sup> n. a.: not available; no full REACH registration; only the highest scoring statements according to CHEM21 (ref. 52) are shown. The lowest figure is given when there is more than one H3xx statement in the highest-scoring category. <sup>b</sup> Scores are based on the order of hazard statement: low hazard (1–3, green); medium hazard (4–6, yellow); high hazard (7–10, red). <sup>c</sup> Key ranking: hazardous (one score of 8 or higher, or two scores between 7 and 10); problematic (one score equal to 7, or two scores between 4 and 6); recommended (all other solvents).



Green metrics calculations were performed to evaluate the credentials of using the sustainable solvents (TMO and DEDMO) in the extraction of hentriacontane-14,16-dione from wheat straw wax and comparison with four solvent systems previously described in the literature (petroleum ether, cyclohexane, *p*-cymene, and CPME).<sup>29</sup> These calculations included process mass intensity (PMI), environmental factor (E-factor), solvent intensity (SI), and water intensity (WI) (Table 3 and Fig. 1, see ESI† for the definitions of metrics and calculations).<sup>54–68</sup> The E-factor and PMI are two elements of the same idea, with the E-factor placing more emphasis on waste minimization and the former on resource usage optimization.

Overall, the process developed in this current work demonstrates significantly better yield, PMI, E-factor, SI, and WI, compared to the previously published process.<sup>29</sup> Although the process developed in this current work which utilized petroleum ether demonstrated the most favourable green metrics, it still demonstrates significant issues, as it is dangerous, non-renewable and petroleum-based solvent, which may cause genetic defects and even cancer.<sup>69</sup> As such, TMO and DEDMO are promising sustainable and potentially bio-based alternatives to traditional toxic non-polar solvents such as petroleum ether and toluene for the extraction of hentriacontane-14,16-dione from wheat straw wax.

### 3.2. Morphological characterization of self-assembly wax and $\beta$ -diketone by different solvents

Fig. 2 and 3 show the scanning electron microscope (SEM) micrograph of deposited unrefined wheat straw wax or the isolated  $\beta$ -diketone by using different solvents including petroleum ether, toluene, TMO, and DEDMO. SEM analysis revealed that the structure of the deposited unrefined wheat straw wax depended on different solvents utilized (Fig. 2). The recrystallized wax by petroleum ether primarily exhibited a folded wax film, while platelets with some tubules were formed when recrystallized by toluene. In the case of TMO, wax formed irregular and flat tubules (Fig. 2c). While using DEDMO led to molecular self-assembly of nano-structured tubules across the entire surface (Fig. 2d). The diameter and length of  $\beta$ -diketone self-assembly of nano-structured tubules produced through the application of DEDMO vary from 0.1 to 0.3  $\mu\text{m}$  (average value of 0.3  $\mu\text{m}$ ) and 0.5 to 4.1  $\mu\text{m}$  (average value of 1.8  $\mu\text{m}$ ), respectively

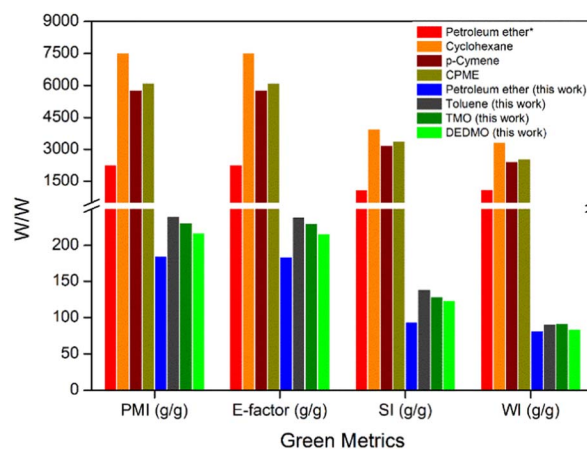


Fig. 1 Green metrics (PMI, E-factor, SI, and WI) for literature process and the processes developed in this work. \* based on Asemave *et al.*<sup>29</sup>

(Fig. 4a and b). These dimensions were consistent with previously reported  $\beta$ -diketone structures.<sup>47,49,70</sup> It is conceivable that the solvents and/or the waxes' have inherent chemical and physical characteristics have an impact on the formation of self-assembled nano-structures.<sup>37,44,48,49</sup> According to Bhushan report,<sup>37</sup> the wax mixture of *Leymus arenarius* which contains hentriacontane-14,16-dione formed tubules when non-polar chloroform was used but formed no tubules when the polar solvent such as ethanol was utilized. Since numerous distinct interactions, such as hydrogen bonds,  $\pi$ -interactions, or van der Waals forces, can be involved, it is difficult to understand the exact nature of the molecular interactions between the solvent and the wax molecules.<sup>37</sup> However, non-polar solvents are known to promote the enol-form of the  $\beta$ -diketone, while more polar solvents would decrease the enolization and favour keto form.<sup>28,29</sup> Thus enolization may play a key role in  $\beta$ -diketone self-assembly of nano-structured tubules in solvents.

$\beta$ -Diketone can typically form tubules in artificial systems.<sup>37,44,48,49,71</sup> Meusel *et al.*<sup>49</sup> have conducted extensive research on the connections between tubule development and the molecular structure of  $\beta$ -diketones, such as hentriacontane-14,16-dione. Huth *et al.*<sup>71</sup> also demonstrated tubule structures made of pure hentriacontane-14,16-dione isolated from barley (*Hordeum vulgare* L.), but they also discovered that, particularly

Table 3 Green metrics (PMI, E-factor, SI, and WI) for the literature process and the processes developed in this work

| Process                       | Recovery yield (%) | PMI (g g <sup>-1</sup> ) | E-factor (g g <sup>-1</sup> ) | SI (g g <sup>-1</sup> ) | WI (g g <sup>-1</sup> ) |
|-------------------------------|--------------------|--------------------------|-------------------------------|-------------------------|-------------------------|
| Petroleum ether <sup>a</sup>  | 18.0               | 2292                     | 2291                          | 1106                    | 1111                    |
| Cyclohexane <sup>a</sup>      | 6.0                | 7516                     | 7515                          | 3960                    | 3333                    |
| <i>p</i> -Cymene <sup>a</sup> | 8.2                | 5790                     | 5789                          | 3188                    | 2439                    |
| CPME <sup>a</sup>             | 7.8                | 6110                     | 6109                          | 3375                    | 2564                    |
| Petroleum ether <sup>b</sup>  | 24.4               | 185                      | 184                           | 94                      | 82                      |
| Toluene <sup>b</sup>          | 21.9               | 240                      | 239                           | 139                     | 91                      |
| TMO <sup>b</sup>              | 21.8               | 231                      | 230                           | 129                     | 92                      |
| DEDMO <sup>b</sup>            | 23.7               | 217                      | 216                           | 124                     | 84                      |

<sup>a</sup> Based on Asemave report.<sup>29</sup> <sup>b</sup> This work.



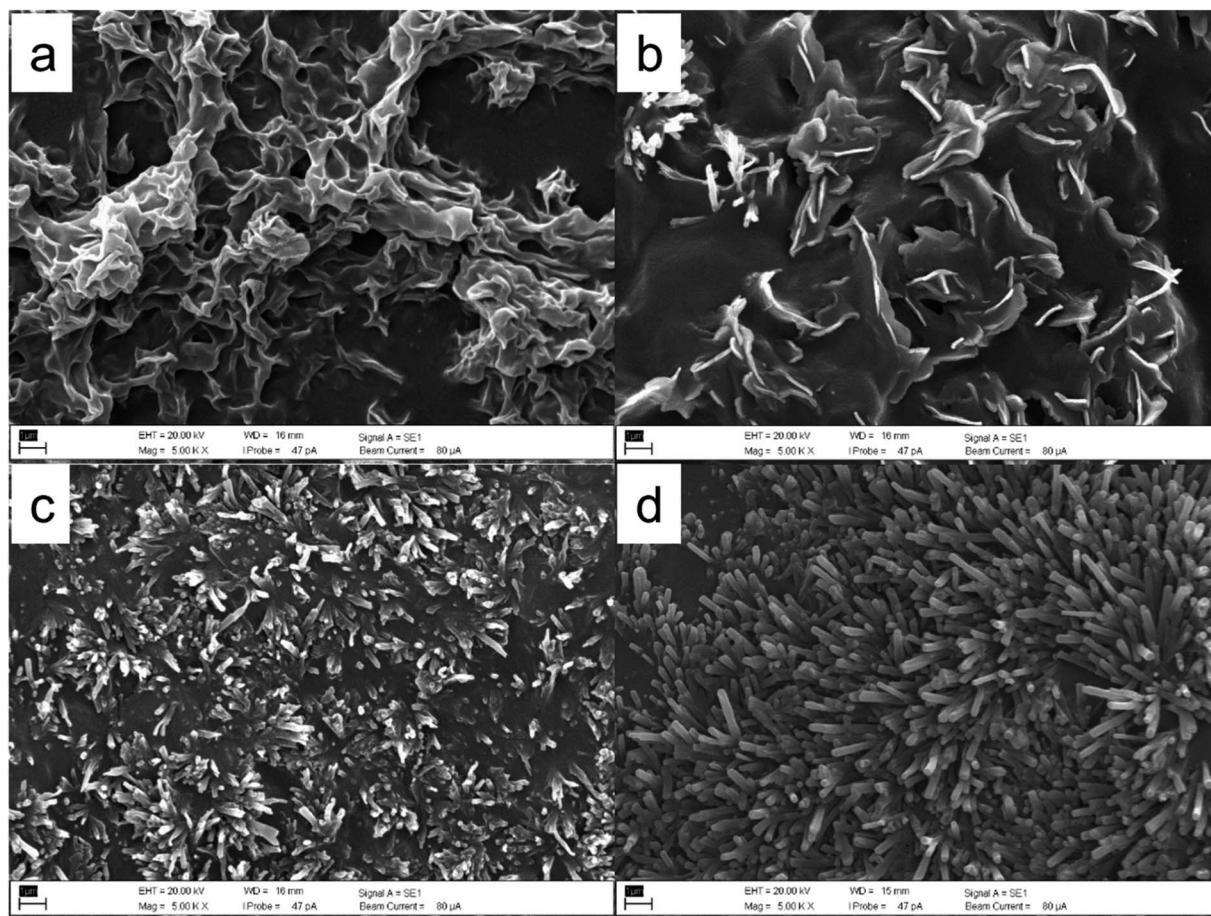


Fig. 2 SEM micrographs of wheat straw wax recrystallized by different solvents, (a) petroleum ether, (b) toluene, (c) TMO, and (d) DEDMO. Scale bars: 1  $\mu\text{m}$ .

in regions with substantial mass accumulation, platelet-shaped and multilayer structures may also form. In addition, recrystallization of  $\beta$ -diketones with C14 and C16 substitutions resulted in the formation of tubules. However,  $\beta$ -diketones that were substituted at positions prior to C12 recrystallized as coiled tubules.<sup>49</sup> This was also true for the tubule formation of  $\beta$ -diketone (hentriacontane-14,16-dione) from wheat straw wax with various solvents in this work, with the exception of toluene that did not demonstrate tubule formation in the wax films (Fig. 3). Although some solvents can lead to the molecular self-assembly of  $\beta$ -diketone into nano-structured tubules, differences were observed in the structure, abundance, and arrangement. Recrystallization or deposition of  $\beta$ -diketone by petroleum ether provided tubule structure in spherulite-like aggregates form on the surface of wax platelets (Fig. 2a). Due to the low boiling point of petroleum ether (40–60  $^{\circ}\text{C}$ ), which causes almost instantaneous solvent evaporation, the  $\beta$ -diketone tubules grow rapidly. This arrangement is characteristic of the kinetic control of deposition, in which the rate of nano-structured growth is limited by the diffusion of molecules from the solution to the deposition surface. Under these circumstances, some spots on the developing structure receive a preference for molecule attachment over others. As a result,

some of the deposition surfaces develop more quickly than others, creating highly anisotropic nano-structure habits that mostly span one dimension.<sup>44</sup> Tubules of  $\beta$ -diketone generated through molecular self-assembly in TMO were randomly distributed, which was consistent with the deposition of unrefined wax (Fig. 3c), however, they did exhibit a greater degree of uniform tubule than the deposited unrefined wax. DEDMO still provided excellent molecular self-assembly of nano-structured tubules, with the uniform shape of the  $\beta$ -diketone (Fig. 3d) with similar dimensions to  $\beta$ -diketone tubules of deposited unrefined wax and also previously reported structures (Fig. 4c and d).<sup>47,49,70</sup> Thermodynamic process contributes to the self-assembly state when using a high boiling point solvent such as DEDMO. The growth on the surface is not limited by the supply of molecules, and there is no distinction between the various sites of attachment. Energy barriers for the adsorption and desorption of molecules on the surface are negligible and the transport rate of molecules diffusing on the surface exceeds the rate of tubule development. As a result, the molecules are bonded to the developing structure at all potential locations and in favourable thermodynamic orientations.<sup>44</sup>

Ensikat *et al.*<sup>72</sup> reported that the hydroxy group of secondary alcohols such as nonacosan-10-ol and nonacosanediol plays



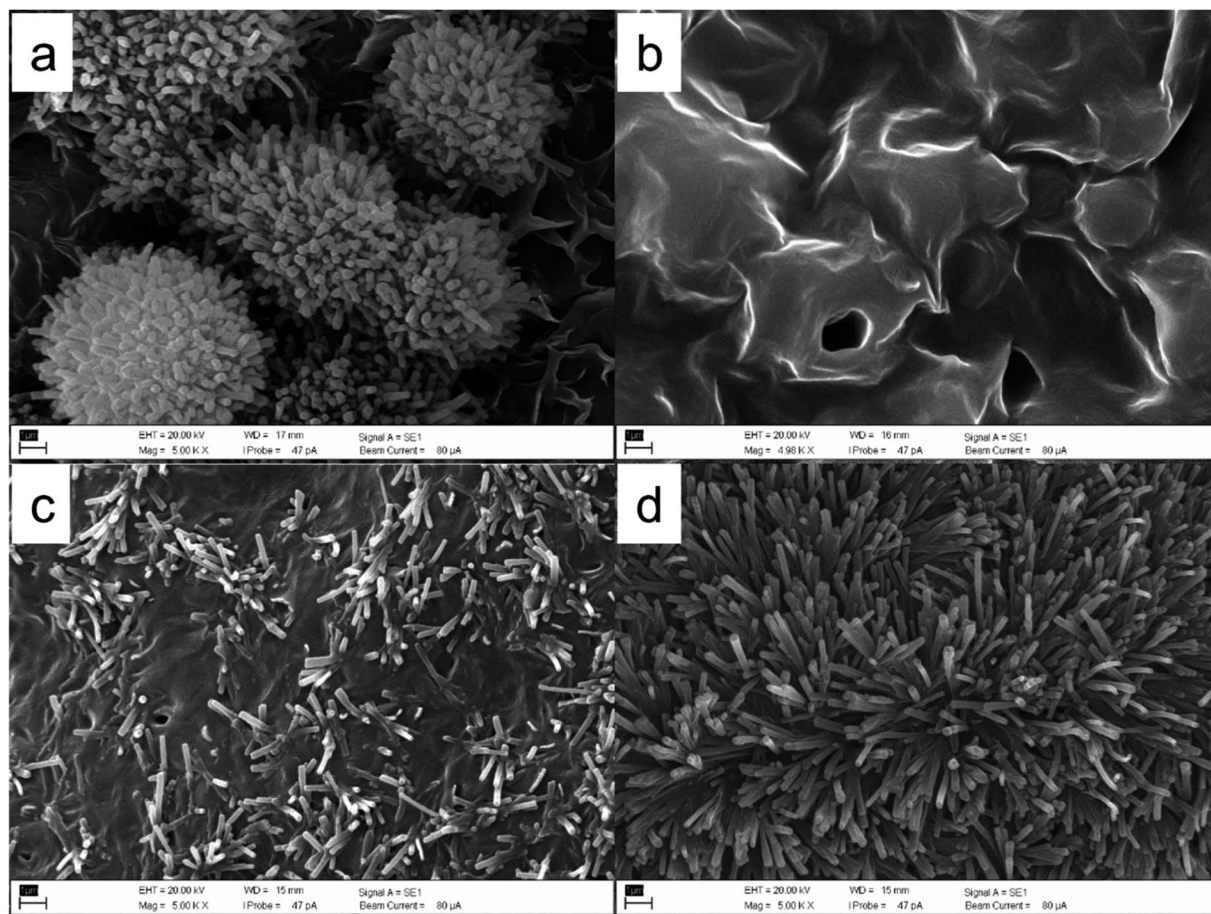


Fig. 3 SEM micrographs of hentriacontane-14,16-dione recrystallized by different solvents, (a) petroleum ether, (b) toluene, (c) TMO, and (d) DEDMO. Scale bars: 1  $\mu\text{m}$ .

an important role in the formation of tubule structure with two effects including hydrogen bonding and inhibition of a tight package because they contain lateral oxygen atoms, resulting in strong curvature and form tubules with a circular cross-section. To represent the primary building blocks, hydrogen bonds are formed when the hydroxyl and ketone groups of two consecutive rows of diketone are pointed in the same direction (Fig. 5). Likewise, in this work, the tubule formation of  $\beta$ -diketone could be impacted by the solvent's ability to promote the tautomerisation equilibrium of  $\beta$ -diketone which showed the relationship with the Kamlet-Taft parameter of a combined measure of dipolarity and polarizability ( $\pi^*$ ) as low  $\pi^*$  can encourage the enol form of  $\beta$ -diketone.<sup>58</sup> Toluene showed a low performance to promote enol form due to its moderate  $\pi^*$  of 0.51 (Table S2<sup>†</sup>),<sup>50,51</sup> resulting in no tubule structure formed. TMO shared similar properties with toluene, however, it provided greater tubule formation than toluene according to its lower  $\pi^*$  of 0.35 (Table S2<sup>†</sup>).<sup>50,51</sup> DEDMO revealed a lower  $\pi^*$  value (0.31, Table S2<sup>†</sup>)<sup>51</sup> than TMO leading to providing better molecular self-assembly of nano-structured tubules. Although petroleum ether contains a mixture of aliphatic hydrocarbons, which showed a significant low  $\pi^*$  ( $-0.16$ , Table S2<sup>†</sup>) and provided tubule structure for  $\beta$ -diketone, it cannot provide tubule

structure for unrefined wheat straw wax. This is due to the component in the mixture also interacting with other components in the wax. As such, DEDMO could be a better solvent for growing the tubule structures of both unrefined wax and the isolated  $\beta$ -diketone.

### 3.3. Hydrophobic study of wheat straw wax and $\beta$ -diketone

To study the effect of hydrophobicity produced by the unrefined wheat straw wax and  $\beta$ -diketone structures in different solvents, water contact angles were measured. Wheat straw wax and isolated  $\beta$ -diketone were dissolved in different solvents at a concentration of 1% w/v and heated at 50  $^{\circ}\text{C}$  for 15 min. After complete dissolution, the solution became pale yellow and transparent. A glass slide was then submerged in the solution, taken out, and allowed to air dry. Once dry, the water contact angle of recrystallized wheat straw wax and  $\beta$ -diketone was measured by the static sessile drop method with a 10  $\mu\text{L}$  deionized water droplet. The median values and standard deviation for all measurements are shown in Fig. 6. The contact angle of water on glass slide without wheat straw wax or  $\beta$ -diketone modification are shown in Table S3<sup>†</sup> and demonstrate significantly lower contact angles of 59 $^{\circ}$ . Overall, recrystallized  $\beta$ -diketone with different solvents demonstrated greater water



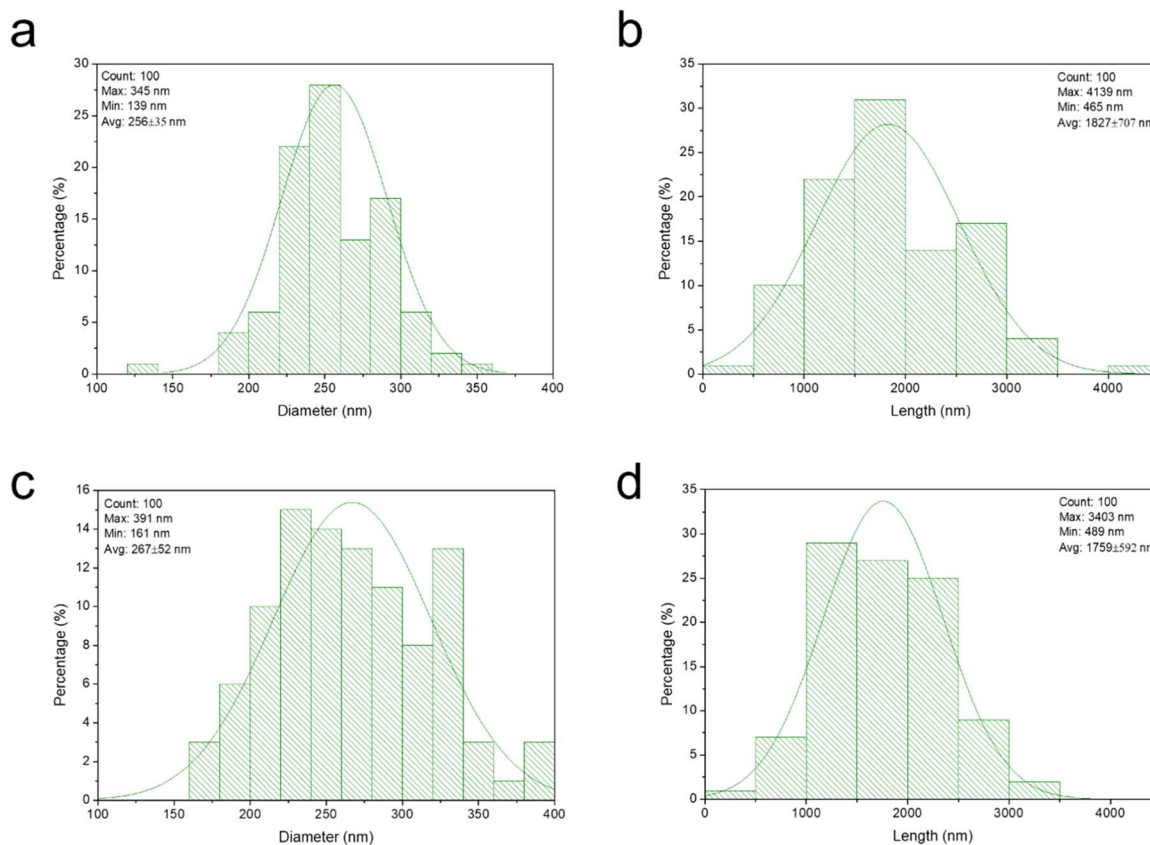


Fig. 4 Size distributions of  $\beta$ -diketone tubules of recrystallized wax (a and b) and isolated  $\beta$ -diketone (c and d) by DEDMO.

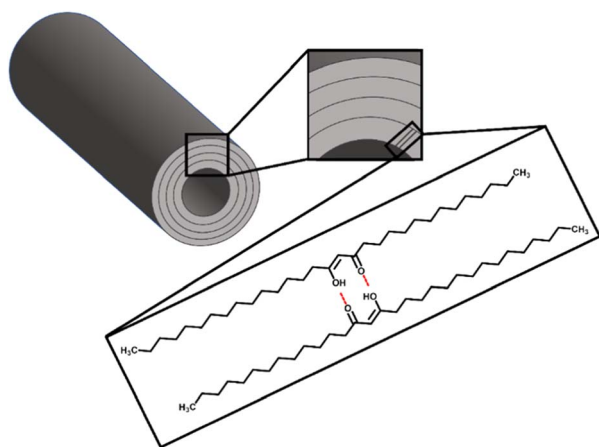


Fig. 5 Proposed model of a nano-structure tubule composed of layers of  $\beta$ -diketone according to Jetter *et al.*<sup>44</sup> and Ensikat *et al.*<sup>70</sup>

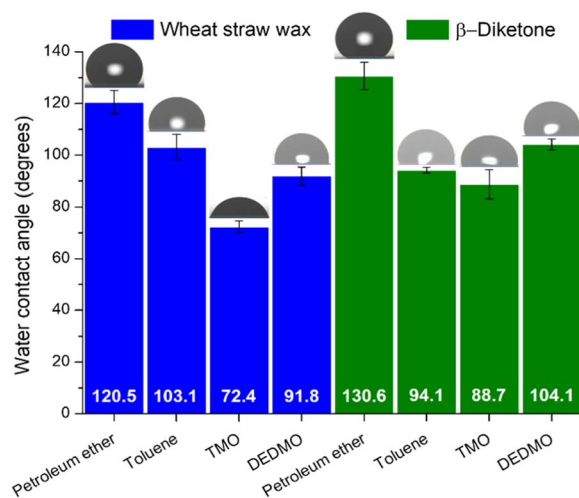


Fig. 6 Water contact angle measurement for wheat straw wax and  $\beta$ -diketone recrystallized by different solvents.

contact angles than those obtained from the unrefined wheat straw wax, except for recrystallization by toluene. The highest water contact angle of  $130.6^\circ$  was found for the recrystallization of  $\beta$ -diketone and  $120.5^\circ$  for wheat straw wax coating by petroleum ether, while the lowest water contact angle of  $88.7^\circ$  and  $72.4^\circ$  for  $\beta$ -diketone and unrefined wax coating by TMO, respectively. Superhydrophobic surfaces are those on which an applied droplet has a contact angle of  $150^\circ$  or greater, while

hydrophobic surfaces have contact angles between  $90^\circ$  and less than  $150^\circ$ .<sup>34–36,38,40,73,74</sup> The leaves of the lotus plant (*Nelumbo nucifera*), which have a very high contact angle of  $164^\circ$  and an inherent hierarchical structure made of convex cell papillae and randomly aligned hydrophobic wax tubules, serve as a model surface for superhydrophobicity and drag reduction.<sup>34,41–43</sup> Wax





self-assembly on plants results in fractal surface roughness, which is assumed to be beneficial for superhydrophobicity.<sup>41</sup> Air pockets exist between the applied water droplet and the surface on rough surfaces where the droplet cannot fully enter the structural grooves. The liquid's surface contact area is decreased by the air pockets in the grooves beneath it.<sup>36,37,72</sup> For the petroleum ether, folded wax film (Fig. 2a) provided a high water contact angle of 120.5° due to its roughness but the water contact angle increased to 130.6° for  $\beta$ -diketone. This is likely due to the formation of spherulite-like aggregates of the tubule can increase the roughness that reduced the water contact area with air pockets. Although the platelet structure of unrefined wheat straw wax recrystallized by toluene provided roughness, the overall surface still demonstrated flat areas that increase the water contact area with a lower water contact angle of 103.1°. For recrystallized  $\beta$ -diketone (Fig. 3b), the roughness was reduced leading to the reduction of water contact angle. Both samples of unrefined recrystallized wheat straw wax and  $\beta$ -diketone from TMO showed a flat structure on the surface and much lower water contact angles than other tested samples (Fig. 2c and 3c). In this case, the recrystallized wheat straw wax and  $\beta$ -diketone structures are too small to capture considerable air and can be regarded as flat surfaces. DEDMO formed tubule structures with random orientation with both recrystallized wheat straw wax and  $\beta$ -diketone. Unlike TMO the surface of the self-assembly of nano-structured tubules was not flat, thus providing a greater water contact angle (Fig. 2d and 3d). Although  $\beta$ -diketone contains polar ketone or hydroxy parts in its molecule, these polar parts can be concealed in the layer of tubule structure, resulting in only nonpolar methyl groups on the layer surface that correlate with hydrophobic properties.<sup>72</sup> The results suggested a hydrophobic property of wheat straw wax and  $\beta$ -diketone; however, this depended on the solvent coating. As such, these preliminary studies show tremendous promise, and further work will refine the technique to produce superhydrophobic coatings for use in a variety of applications.

## 4. Conclusions

It has been demonstrated that a natural hydrophobic molecule  $\beta$ -diketone, with potential industrial applications in chelation or coatings, namely hentriacontane-14,16-dione, could be selectively extracted from wheat straw wax using sustainable and potentially bio-based solvents (TMO and DEDMO) with improvement recovery yield, as compared with previously reported methodology (reduction ten times of solvents and chemical utilization). This is the first application of solvents such as DEDMO in extraction of natural products. Compared to their petrochemical counterparts, bio-based and sustainable solvents offer several benefits including renewability, and great ecological aspects (*i.e.*, low ecotoxicity and low toxicity toward humans). Additionally, DEDMO showed an excellent impact on the self-assembly of nano-structured tubule formation on both wax and  $\beta$ -diketone. This solvent also affected the hydrophobicity of both wax and  $\beta$ -diketone correlated with their nano-structure formation and orientation. Moreover, in terms of green chemistry metrics analysis, the use of the developed

methodology proved greater advantages than previously published technique reports, due to its high product yield and significantly lower waste generation. As part of a holistic bio-refinery, this technique may develop new possibilities for the selective extraction and purification of hentriacontane-14,16-dione utilizing green solvents from wheat straw wax. Finally, valuing wheat straw waste would help to solve the issue of considerable accumulation of excess biomass wastes from agriculture.

## Conflicts of interest

There are no conflicts to declare.

## Acknowledgements

This research was supported by the Fundamental Fund of Khon Kaen University. Research on "Valorisation of industrial food wastes for the development of sustainable products towards a bio-based circular economy" by Khon Kaen University, Department of Chemistry, has received funding support from the National Science, Research and Innovation Fund. This project is funded by National Research Council of Thailand (NRCT) (grant number: N42A650240). Mr Suwivat Sangon would like to thank the support of Institute for the Promotion of Teaching Science and Technology for his Development and Promotion of Science and Technology Talents Project scholarship. The Center of Excellence for Innovation in Chemistry (PERCH-CIC), Ministry of Higher Education, Science, Research and Innovation is also gratefully acknowledged.

## References

- 1 V. L. Budarin, P. S. Shuttleworth, J. R. Dodson, A. J. Hunt, B. Lanigan, R. Marriott, K. J. Milkowski, A. J. Wilson, S. W. Breeden, J. Fan, E. H. K. Sin and J. H. Clark, *Energy Environ. Sci.*, 2011, **4**, 471–479.
- 2 J. H. Clark, V. Budarin, F. E. I. Deswarte, J. J. E. Hardy, F. M. Kerton, A. J. Hunt, R. Luque, D. J. Macquarrie, K. Milkowski, A. Rodriguez, O. Samuel, S. J. Tavener, R. J. White and A. J. Wilson, *Green Chem.*, 2006, **8**, 853–860.
- 3 T. M. Attard, A. J. Hunt, A. S. Matharu, J. A. Houghton and I. Polikarpov, in *Introduction to Chemicals from Biomass*, John Wiley & Sons, Ltd, 2015, pp. 31–52.
- 4 F. E. I. Deswarte, J. H. Clark, A. J. Wilson, J. J. E. Hardy, R. Marriott, S. P. Chahal, C. Jackson, G. Heslop, M. Birkett, T. J. Bruce and G. Whiteley, *Biofuels, Bioprod. Biorefin.*, 2007, **1**, 245–254.
- 5 J. Copeland, D. Turley, S. Hutton, *National and regional supply/demand balance for agricultural straw in Great Britain*, National Non-Food Crops Centre, 2008, p. 17.
- 6 A. G. Marangoni and E. Daniel Co, *J. Am. Oil Chem. Soc.*, 2012, **89**, 749–780.
- 7 J. C. del Río, P. Prinsen and A. Gutiérrez, *J. Agric. Food Chem.*, 2013, **61**, 1904–1913.
- 8 F. E. I. Deswarte, J. H. Clark, J. J. E. Hardy and P. M. Rose, *Green Chem.*, 2006, **8**, 39–42.



- 9 E. H. K. Sin, R. Marriott, A. J. Hunt and J. H. Clark, *C. R. Chim.*, 2014, **17**, 293–300.
- 10 L. L. Jackson, *Phytochemistry*, 1971, **10**, 487–490.
- 11 Y. Athukorala, G. Mazza and B. D. Oomah, *Eur. J. Lipid Sci. Technol.*, 2009, **111**, 705–714.
- 12 A. P. Tulloch and L. L. Hoffman, *Lipids*, 1974, **9**, 219.
- 13 D. Canizares, P. Angers and C. Ratti, *Ind. Crops Prod.*, 2019, **141**, 111700.
- 14 G. Bianchi and M. Corbellini, *Phytochemistry*, 1977, **16**, 943–945.
- 15 A. P. Tulloch and R. O. Weenink, *Can. J. Chem.*, 1969, **47**, 3119–3126.
- 16 A. P. Tulloch and L. L. Hoffman, *Phytochemistry*, 1971, **10**, 871–876.
- 17 A. P. Tulloch and L. L. Hoffman, *Phytochemistry*, 1973, **12**, 2217–2223.
- 18 n-Hexane - Substance Information - ECHA, <https://echa.europa.eu/substance-information/-/substanceinfo/100.003.435>, accessed November 21, 2022.
- 19 O. US EPA, Initial List of Hazardous Air Pollutants with Modifications, <https://www.epa.gov/haps/initial-list-hazardous-air-pollutants-modifications>, accessed November 21, 2022.
- 20 L. Wang, C. L. Weller, V. L. Schlegel, T. P. Carr and S. L. Cuppett, *Eur. J. Lipid Sci. Technol.*, 2007, **109**, 567–574.
- 21 W. H. Morrison, R. Holser and D. E. Akin, *Ind. Crops Prod.*, 2006, **24**, 119–122.
- 22 Y. Athukorala, F. S. Hosseinian and G. Mazza, *LWT-Food Sci. Technol.*, 2010, **43**, 660–665.
- 23 L. Wang and C. L. Weller, *Trends Food Sci. Technol.*, 2006, **17**, 300–312.
- 24 Y. Athukorala and G. Mazza, *Ind. Crops Prod.*, 2010, **31**, 550–556.
- 25 P. Noppawan, A. G. Lanctôt, M. Magro, P. G. Navarro, N. Supanchaiyamat, T. M. Attard and A. J. Hunt, *BMC Chem.*, 2021, **15**, 37.
- 26 E. H. K. Sin, PhD thesis, University of York, 2012, <https://etheses.whiterose.ac.uk/3123/>, accessed November 21, 2022.
- 27 W. Fu, Q. Chen, H. Hu, C. Niu and Q. Zhu, *Sep. Purif. Technol.*, 2011, **80**, 52–58.
- 28 K. Asemave, F. Byrne, T. J. Farmer, J. H. Clark and A. J. Hunt, *RSC Adv.*, 2016, **6**, 95789–95792.
- 29 K. Asemave, PhD thesis, University of York, 2016, <https://etheses.whiterose.ac.uk/14254/>, accessed November 21, 2022.
- 30 J. R. Dodson, A. J. Hunt, H. L. Parker, Y. Yang and J. H. Clark, *Chem. Eng. Process.*, 2012, **51**, 69–78.
- 31 N. Supanchaiyamat and A. J. Hunt, *ChemSusChem*, 2019, **12**, 397–403.
- 32 S. Pechook and B. Pokroy, *Adv. Funct. Mater.*, 2012, **22**, 745–750.
- 33 A. Niemietz, K. Wandelt, W. Barthlott and K. Koch, *Prog. Org. Coat.*, 2009, **66**, 221–227.
- 34 K. Koch, B. Bhushan, Y. C. Jung and W. Barthlott, *Soft Matter*, 2009, **5**, 1386–1393.
- 35 Y. C. Jung and B. Bhushan, *Langmuir*, 2009, **25**, 9208–9218.
- 36 B. Bhushan, Y. C. Jung and K. Koch, *Langmuir*, 2009, **25**, 3240–3248.
- 37 B. Bhushan, Y. C. Jung, A. Niemietz and K. Koch, *Langmuir*, 2009, **25**, 1659–1666.
- 38 B. Bhushan, Y. C. Jung and K. Koch, *Philos. Trans. R. Soc.*, 2009, **367**, 1631–1672.
- 39 K. Koch, A. Dommissé and W. Barthlott, *Cryst. Growth Des.*, 2006, **6**, 2571–2578.
- 40 K. Koch, K. D. Hartmann, L. Schreiber, W. Barthlott and C. Neinhuis, *Environ. Exp. Bot.*, 2006, **56**, 1–9.
- 41 K. Koch, B. Bhushan and W. Barthlott, *Prog. Mater. Sci.*, 2009, **54**, 137–178.
- 42 W. Barthlott and C. Neinhuis, *Planta*, 1997, **202**, 1–8.
- 43 K. Koch, B. Bhushan and W. Barthlott, *Soft Matter*, 2008, **4**, 1943–1963.
- 44 R. Jetter and M. Riederer, *Planta*, 1994, **195**, 257–270.
- 45 R. Jetter and M. Riederer, *Bot. Acta*, 1995, **108**, 111–120.
- 46 K. Koch, C. Neinhuis, H.-J. Ensikat and W. Barthlott, *J. Exp. Bot.*, 2004, **55**, 711–718.
- 47 C. E. Jeffree, E. A. Baker and P. J. Holloway, *New Phytol.*, 1975, **75**, 539–549.
- 48 I. Meusel, C. Neinhuis, C. Markstädter and W. Barthlott, *Can. J. Bot.*, 1999, **77**, 706–720.
- 49 I. Meusel, C. Neinhuis, C. Markstädter and W. Barthlott, *Plant Biol.*, 2000, **2**, 462–470.
- 50 F. Byrne, B. Forier, G. Bossaert, C. Hoebbers, T. J. Farmer, J. H. Clark and A. J. Hunt, *Green Chem.*, 2017, **19**, 3671–3678.
- 51 P. Noppawan, S. Sangon, N. Supanchaiyamat, J. Sherwood and A. J. Hunt, *ACS Sustainable Chem. Eng.*, 2022, **10**, 4486–4493.
- 52 D. Prat, A. Wells, J. Hayler, H. Sneddon, C. R. McElroy, S. Abou-Shehada and P. J. Dunn, *Green Chem.*, 2015, **18**, 288–296.
- 53 Guidance for Annex V-Exemption from the obligation to register, [https://echa.europa.eu/documents/10162/23036412/annex\\_v\\_en.pdf](https://echa.europa.eu/documents/10162/23036412/annex_v_en.pdf), accessed February 18, 2021.
- 54 S. Abou-Shehada, P. Mampuy, B. U. W. Maes, J. H. Clark and L. Summerton, *Green Chem.*, 2017, **19**, 249–258.
- 55 N. J. Willis, C. A. Fisher, C. M. Alder, A. Harsanyi, L. Shukla, J. P. Adams and G. Sandford, *Green Chem.*, 2016, **18**, 1313–1318.
- 56 T. V. T. Phan, C. Gallardo and J. Mane, *Green Chem.*, 2015, **17**, 2846–2852.
- 57 C. R. McElroy, A. Constantinou, L. C. Jones, L. Summerton and J. H. Clark, *Green Chem.*, 2015, **17**, 3111–3121.
- 58 P. Noppawan, S. Sangon, N. Supanchaiyamat and A. J. Hunt, *Green Chem.*, 2021, **23**, 5766–5774.
- 59 F. Roschangar, R. A. Sheldon and C. H. Senanayake, *Green Chem.*, 2015, **17**, 752–768.
- 60 C. Jiménez-González, D. J. C. Constable and C. S. Ponder, *Chem. Soc. Rev.*, 2012, **41**, 1485–1498.
- 61 C. Jimenez-Gonzalez, C. S. Ponder, Q. B. Broxterman and J. B. Manley, *Org. Process Res. Dev.*, 2011, **15**, 912–917.
- 62 J. Augé, *Green Chem.*, 2008, **10**, 225–231.
- 63 J. Andraos, *Org. Process Res. Dev.*, 2005, **9**, 149–163.
- 64 D. J. C. Constable, A. D. Curzons and V. L. Cunningham, *Green Chem.*, 2002, **4**, 521–527.



## Paper

- 65 X. Zhang, X. Ma, W. Qiu, J. Evans and W. Zhang, *Green Chem.*, 2019, **21**, 349–354.
- 66 A. Muthengi, X. Zhang, G. Dhawan, W. Zhang, F. Corsini and W. Zhang, *Green Chem.*, 2018, **20**, 3134–3139.
- 67 J. Martínez, J. F. Cortés and R. Miranda, *Processes*, 2022, **10**, 1274.
- 68 M. A. Droesbeke and F. E. Du Prez, *ACS Sustainable Chem. Eng.*, 2019, **7**, 11633–11639.
- 69 Petroleum ether – Safety data sheet, <https://www.fishersci.com/msdsproxy%3FproductName%3DP4804%26productDescription%3DPET%2BETHER%2BPESTICIDE%2BCERT%2B4L%26catNo%3DP4804%26vendorId%3DVN00033897%26storeId%3D10652>, accessed November 22, 2022.
- 70 H. J. Ensikat, M. Boese, W. Mader, W. Barthlott and K. Koch, *Chem. Phys. Lipids*, 2006, **144**, 45–59.
- 71 M. A. Huth, A. Huth and K. Koch, *Beilstein J. Nanotechnol.*, 2021, **12**, 939–949.
- 72 H. J. Ensikat, P. Ditsche-Kuru, C. Neinhuis and W. Barthlott, *Beilstein J. Nanotechnol.*, 2011, **2**, 152–161.
- 73 Y. C. Jung and B. Bhushan, *ACS Nano*, 2009, **3**, 4155–4163.
- 74 C. W. Extrand, *Langmuir*, 2002, **18**, 7991–7999.

